The Role of Glu39 in Mn^{II} Binding and Oxidation by Manganese Peroxidase from *Phanerochaete chrysoporium*†

Heather L. Youngs,‡ Maarten D. Sollewijn Gelpke,‡ Dongmei Li,‡ Munirathinam Sundaramoorthy,§ and Michael H. Gold*,‡

Department of Biochemistry and Molecular Biology, Oregon Graduate Institute of Science and Technology, Portland, Oregon 97291-1000, and Department of Biochemistry and Molecular Biology, University of Kansas Medical Center, Kansas City, Kansas 66160

Received September 7, 2000; Revised Manuscript Received December 21, 2000

ABSTRACT: Manganese peroxidase (MnP) is a heme-containing enzyme produced by white-rot fungi and is part of the extracellular lignin degrading system in these organisms. MnP is unique among Mn binding enzymes in its ability to bind and oxidize Mn^{II} and efficiently release Mn^{III}. Initial site-directed mutagenesis studies identified the residues E35, E39, and D179 as the Mn binding ligands. However, an E39D variant was recently reported to display wild-type Mn binding and rate of oxidation, calling into question the role of E39 as an Mn ligand. To investigate this hypothesis, we performed computer modeling studies which indicated metal−ligand bond distances in the E39D variant and in an E35D−E39D−D179E triple variant which might allow Mn binding and oxidation. To test the model, we reconstructed the E35D and E39D variants used in the previous study, as well as an E39A single variant and the E35D−E39D−D179E triple variant of MnP isozyme 1 from *Phanerochaete chrysosporium*. We find that all of the variant proteins are impaired for Mn^{II} binding (K_m increases 20−30-fold) and Mn^{II} oxidation (k_{cat} decreases 50−400-fold) in both the steady state and the transient state. In particular, mutation of the E39 residue in MnP decreases both Mn binding and oxidation. The catalytic efficiency of the E39A variants decreased $\sim 10^4$-fold, while that of the E39D variant decreased $\sim 10^3$-fold. Contrary to initial modeling results, the triple variant performed only as well as any of the single Mn ligand variants. Interestingly, the catalytic efficiency of the triple variant decreased only 10^4-fold, which is $\sim 10^2$-fold better than that reported for the E35Q−D179N double variant. These combined studies indicate that precise geometry of the Mn ligands within the Mn binding site of MnP is essential for the efficient binding, oxidation, and release of Mn by this enzyme. The results clearly indicate that E39 is a Mn ligand and that mutation of this ligand decreases both Mn binding and the rate of Mn oxidation.

White-rot fungi are uniquely adapted to degrade lignin, a phenylpropanoid cell wall polymer which provides rigidity, cell adhesion, and microbial resistance to vascular plants (*1, 2*). The best-studied white-rot basidiomycete, *Phanerochaete chrysosporium*, preferentially degrades lignin under nutrient nitrogen limiting (idiophasic) conditions by secreting enzymes, including lignin and manganese peroxidases (LiP[1] and MnP), and a hydrogen peroxide generating system (*3*−*6*). Though specific components of the lignin degrading machinery of various white-rot fungi vary, manganese peroxidases (MnPs) have been detected in virtually all lignin degrading fungi so far studied (*7*−*11*).

P. chrysosporium produces a series of extracellular MnP isozymes under ligninolytic conditions (*12, 13*). MnP isozyme 1 has been purified and studied extensively by a variety of biochemical and biophysical methods (*5, 12, 14*−*16*). Spectroscopic, DNA sequence comparison, and X-ray crystallographic studies indicate that the heme environment of MnP is similar to that of other plant and fungal peroxidases (*17*−*23*). Kinetic and spectroscopic characterization of the native and oxidized intermediates of MnP indicates that the catalytic cycle is similar to that of other plant and fungal peroxidases (*15, 24*). However, MnP is unique among peroxidases in utilizing Mn^{II} as its primary reducing substrate (*14, 15*). The peroxidatic cycle is as follows:

$$MnP + H_2O_2 \rightarrow MnPI\ (Fe^{IV}{=}O^{\bullet+}) + H_2O$$

$$MnPI + Mn^{II} \rightarrow MnPII\ (Fe^{IV}{=}O) + Mn^{III}$$

$$MnPII + Mn^{II} + 2H^+ \rightarrow MnP + H_2O + Mn^{III}$$

where MnPI contains an oxoferryl porphyrin π cation radical (two-electron-oxidized) and MnPII contains an oxoferryl (one-electron-oxidized) heme. Enzyme-generated Mn^{III} is stabilized by dicarboxylic organic acid chelators, such as oxalate (*15, 25, 26*). The Mn^{III}−chelator complex is stable

† This research was supported by Grants MCB-9808430 from the National Science Foundation and DE-FG03-96ER20235 from the U.S. Department of Energy, Office of Basic Energy Sciences (to M.H.G.).

* To whom correspondence should be addressed at the Department of Biochemistry and Molecular Biology, Oregon Graduate Institute of Science and Technology, 20000 N.W. Walker Rd., Beaverton, OR 97006-8921. Telephone: 503-748-1076. Fax: 503-748-1464. E-mail: mgold@bmb.ogi.edu.

‡ Oregon Graduate Institute of Science and Technology.

§ University of Kansas Medical Center.

[1] Abbreviations: CcP, cytochrome *c* peroxidase; FPLC, fast protein liquid chromatography; *gpd*, glyceraldehyde-3-phosphate dehydrogenase gene; HCHN, high carbon−high nitrogen; LiP, lignin peroxidase; *mnp*, manganese peroxidase gene; MnP, manganese peroxidase protein; MnPI, MnP compound I; MnPII, MnP compound II.

10.1021/bi002104s CCC: $20.00
Published on Web 01/26/2001

enough to diffuse from the enzyme and oxidize terminal phenolic substrates, including lignin (*27*) and aromatic pollutants (*28*−*31*). Oxidation of nonphenolic lignin substructures by MnP has been proposed to occur via radical mediators (*32, 33*).

The Mn^{II} binding site of MnP isozyme 1 from *P. chrysosporium* was identified by X-ray crystallographic and initial site-directed mutagenesis studies (*19, 34*−*36*). The MnP crystal structure indicates that enzyme-bound Mn^{II} is hexacoordinate with two water ligands and four carboxylate ligands from heme propionate 6 and three amino acid residues: D179, E35, and E39 (*19*). Several variant MnPs—D179N, E35Q, E39Q, and D179N−E35Q—were created by exchanging the amino acid carboxylate ligands for their respective amides via site-directed mutagenesis of the *mnp1* gene (*34, 35*). The amino acid substitutions were chosen to maintain steric constraints within the site while abolishing Mn^{II} ligation. Binding and oxidation of Mn^{II} were greatly reduced in all of the variant enzymes. In all other respects, including reactivity toward H_2O_2 and substrates with alternate binding sites, the variant enzymes were similar to the wild type, indicating that the mutations specifically affected Mn^{II} binding and oxidation rather than the overall structure or function of the enzyme (*34, 35*). This was confirmed by X-ray crystallographic analysis of the variants, which clearly showed disruption of the Mn binding site while other structural features remained unchanged (*36*).

As a result of these combined studies, D179, E35, and E39 were identified as Mn^{II} ligands. However, a recent mutagenesis study of these ligands has raised doubts regarding the importance of E39 in Mn^{II} binding and oxidation (*37*). In that study, site-directed mutagenesis was used to shorten the alkyl side chains of the E35 and E39 ligands by isochemical substitution to produce E35D and E39D mutant *mnp* genes. A D179A variant was also made. The proteins were then heterologously expressed in *E. coli*, isolated from inclusion bodies, and reconstituted. The D179A and E35D variants exhibited characteristics similar to the previous single variant MnPs (D179N and E35Q), including increased K_m for Mn^{II} and decreased k_{cat} values (*37*). In striking contrast to the previous E39Q variant (*35*), the E39D variant was claimed to exhibit wild-type characteristics including wild-type kinetics for Mn^{II} binding and oxidation under both steady-state and transient-state conditions (*37*). Those investigators concluded that E39 was "not critically important" to Mn^{II} binding nor electron transfer from Mn^{II} to the enzyme. In this paper, we reexamine the role of E39 in Mn^{II} binding and oxidation through computer modeling and steady-state and transient-state kinetic analysis of our own homologously expressed E39D variant as well as a new variant, E39A. We also probe the flexibility of the Mn^{II} binding site in MnP by examining an isochemical triple variant, D179E−E35D−E39D.

EXPERIMENTAL PROCEDURES

Organisms. P. chrysosporium wild-type strain OGC101, auxotropic strain OGC107-1 (Ade1), and prototrophic transformants were maintained as described previously (*38*). *Escherichia coli* DH5α was used for subcloning plasmids.

Molecular Modeling. Structures were modeled using the Swiss PDB Viewer v3.6b3 (Glaxo-Wellcome). The crystal structure data for wild-type MnP were obtained from the Protein Data Bank file 1mnp (*19*). As recommended by the software documentation, ligands and Mn were first manually translated/rotated to avoid steric interactions following introduction of mutation. The structures were then subjected to successive energy minimization using the GROMOS96 protocol (*39*). Structures were then rendered using the POV-Ray for Windows 3.1 g.watcom.win32 rendering engine (Persistence of Vision Development Team).

Construction of Transformation Plasmids. Site-directed mutations were introduced into the pGM1 plasmid (*35*), which contains 1.1 kb of the *gpd* promoter fused to the coding region of *P. chrysosporium mnp1* at the ATG translation initiation codon, by the PCR-based Quikchange (Stratagene) method. Forward and reverse primers (16−20 bp) containing altered codons were obtained to introduce the mutations for each amino acid. The GAG codon for E39 was changed to GAC (E39D) or GCG (E39A). The GAA codon for E35 was changed to GAC (E35D). The triple variant was constructed by successive rounds of the Quikchange protocol. The E39D construct was used to create an E39D−E35D double mutation. Subsequently, the GAC codon of D179 of this double variant was altered to GAG (D179E) to create the E39D−E35D−D179E triple variant. Following mutagenesis, the plasmids were isolated and sequenced in both directions to confirm the mutations and check for any other sequence alterations. Plasmids were double-digested, and the *Xba*I−*Eco*RI fragments, containing the *gpd* promoter and mutated *mnp1* genes, were subcloned into pOGI18 (*38, 40*), a *P. chrysosporium* transformation plasmid containing the *Schizophyllum commune ade5* aminoimidazole ribonucleotide synthetase gene as a selectable marker. The entire *mnp1* coding regions of the resulting plasmids were sequenced to again verify the mutations and to ensure no other sequence alterations occurred.

Transformation of P. chrysosporium. Protoplasts of the Ade^- strain OGC107-1 were transformed as described (*38, 40*−*42*), using 1 μg of *Eco*RI-linearized plasmid as the transforming DNA. Prototrophic transformants were transferred to minimal medium slants to confirm adenine prototrophy and were subsequently assayed for MnP activity using the *o*-anisidine plate assay as described previously (*42*). Transformants exhibiting the highest activity on plates were purified by fruiting as described previously (*43*), and the progeny were rescreened for MnP activity by the plate assay. The purified transformants exhibiting the highest activity in large shaking cultures were selected for further study.

Production and Purification of Variant MnP Proteins. Selected transformants were maintained on MYV slants and grown in high carbon−high nitrogen (HCHN) liquid medium in stationary culture from conidial inocula as described previously (*42*). These stationary cultures were homogenized and used as inocula for shaking cultures containing 1 L of liquid medium in 2-L flasks, and were grown for 3 days at 28 °C. The extracellular medium was filtered and concentrated, and the variant MnP proteins were purified by a combination of Phenyl Sepharose CL-6B hydrophobic interaction, Cibacron blue 3GA dye affinity, and MonoQ anionic exchange chromatographies as described previously (*35, 42*). Purified variant enzyme had Rz values ≥4 and yields of ∼2 $mg \cdot L^{-1}$. The enzyme concentration was

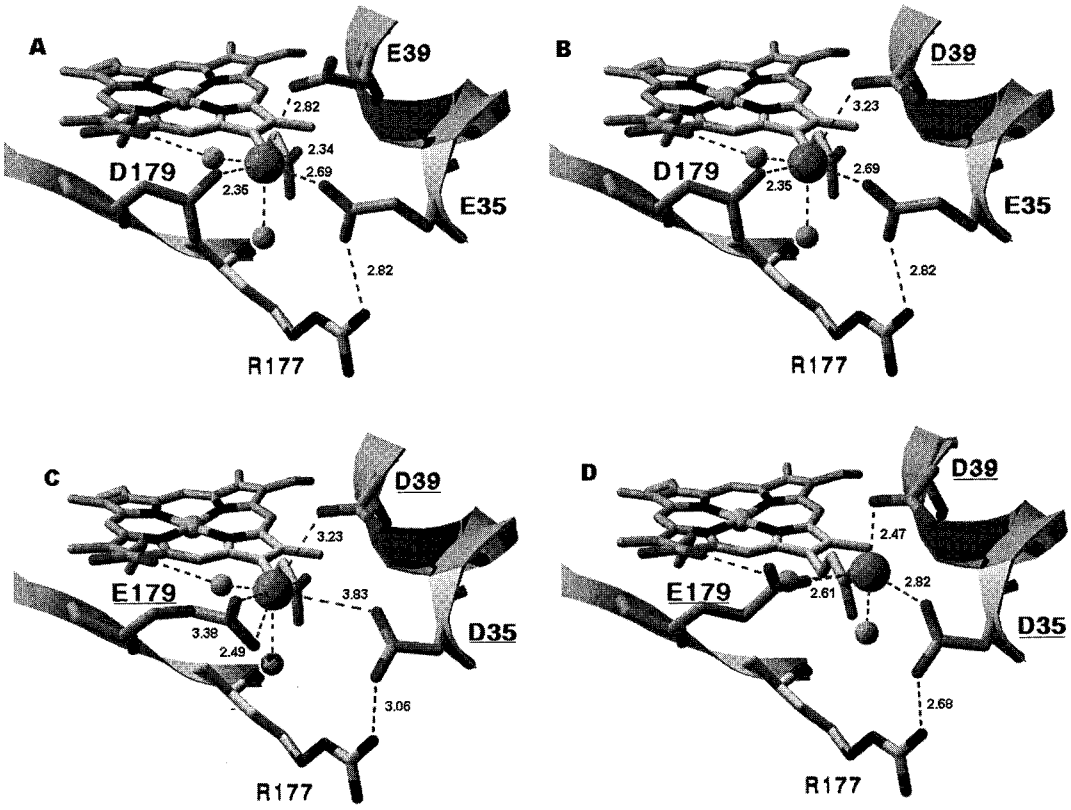

FIGURE 1: (A) Mn^{II} binding site of wild-type manganese peroxidase isozyme 1 from *P. chrysosporium* from X-ray crystal structure data (*19*). Mn^{II} binding sites of the (B) E39D single variant and (C, D) DDE (E39D−E35D−D179E) triple variant could be modeled with either retention of the wild-type geometry (B, C) or optimization of ligand bond distances (D), but not both. Mutated residues are underlined. Mn−ligand distances are reported in angstroms. Structures were modeled using the Swiss PDB Viewer v3.6b3 and POV-Ray for Windows as described.

determined using $\epsilon_{406} = 129\ mM^{-1}\cdot cm^{-1}$ (*12*). Wild-type enzyme was produced as described previously (*44*).

Spectroscopic Procedures and Kinetic Analysis. Electronic absorption spectra and steady-state kinetic analyses were performed using a Shimadzu UV-260 spectrophotometer at room temperature. Steady-state Mn^{II} oxidation was measured as the formation of Mn^{III}-malonate, followed at 270 nm ($\epsilon_{270} = 11.6\ mM^{-1}$) (*15*). Apparent K_m and k_{cat} values for Mn^{II} and H_2O_2 were calculated from Lineweaver−Burk plots. Reaction mixtures contained 0.5 $\mu g\cdot mL^{-1}$ enzyme, 50 mM malonate, pH 4.5, and various concentrations of $MnSO_4$ and H_2O_2, as indicated. Transient-state kinetic experiments were performed using an Applied PhotoPhysics SX.18MV sequential stopped-flow reaction analyzer at 25.0 ± 0.2 °C as described (*45*). Reductions of each intermediate by ferrocyanide were measured individually. Complete formation of enzyme intermediates was confirmed by diode array rapid scanning. All reactions contained 50 mM potassium malonate, pH 4.5, and the ionic strength of all solutions was adjusted to $\mu = 0.1$ M with K_2SO_4. The final concentration of enzyme was 1 μM, and a minimum 10-fold excess of substrate was used in all reactions to ensure pseudo-first-order reaction kinetics. All kinetic traces displayed single-exponential character from which pseudo-first-order rate constants were calculated.

PCR of Genomic DNA. Mycelia from 3-day-old stationary cultures [high carbon−high nitrogen (HCHN)] of the selected E39D transformant were flash-frozen in liquid nitrogen and ground by mortar and pestle. Genomic DNA was extracted as described previously (*18*, *46*). To ensure selective amplification of recombinant *mnp*, primers in both the *gpd* and *mnp* genes were selected. The 19-bp forward primer in the PCR reaction annealed to the *gpd* promoter 75 bp 5′ of the *mnp* ATG (*42*). The 24-bp reverse primer annealed to the first 13 bp of intron IV and 12 bp of exon III in the *mnp1* gene. The resulting 685-bp fragment was purified using the QIAquick PCR purification kit (Qiagen) and sequenced directly.

Chemicals. All chemicals were reagent grade and obtained from Sigma/Aldrich. Solutions for kinetic analyses were prepared with HPLC-grade water.

RESULTS

Computer Modeling of Variant Enzymes. Prior to construction, the variant MnPs were modeled using the Swiss PDB-Viewer. Virtual mutations were introduced into the 2.06-Å crystal structure (*19*). Figure 1A indicates the Mn^{II}−ligand distances for the wild-type protein. Modeling of E39D and the E35D−E39D−D179E variants showed various scenarios in repeated energy minimizations, indicating some variability in the software's ability to predict the most stable conformation. Modeling of the E39D variant indicated some conformations with bond lengths similar to the wild-type but with altered Mn ligand geometry (data not shown). If the wild-type Mn geometry was maintained, the models showed an increase in the Mn−residue 39 bond length to 3.23 Å, indicating probable loss of this ligand from the Mn coordination sphere (Figure 1B). Similarly, modeling of the E35D−E39D−D179E triple variant with wild-type Mn geometry

showed retention of the 179 ligand (with possible bidentate coordination) and loss of the residue 35 and residue 39 ligands (Figure 1C). Shorter bond lengths, suggesting retention of all the ligands, could be obtained for the triple variant, but only with an accompanying distortion of the Mn ligation geometry (Figure 1D). Modeling of the E35D variant showed a 0.8-Å increase in the Mn−residue 35 bond distance (data not shown) from 2.6 Å for E35 to 3.4 Å for D35, suggesting that the D35 residue can no longer function effectively as a Mn ligand.

Expression and Purification of the Variant Enzymes. Prior to the fungal transformation, the entire coding regions of the mutant *mnp1* in the pAGM plasmids were sequenced. The only variations in the sequence versus the wild-type *mnp1* gene were the desired mutations. Transformation of the Ade$^-$ strain (OGC107-1) with the *Eco*RI-linearized plasmids resulted in multiple (10−80) transformants. Typically, 20% of the transformants were positive for MnP activity by the *o*-anisidine plate assay, using 5 mM $MnSO_4$ (*42*). For each mutant, three transformants exhibiting maximal activity on the plate assay were selected and purified by fruiting (*38*, *40*, *43*). Colonies from single basidiospores were rescreened for MnP activity by the plate assay, and three purified isolates for each mutant were then grown in large HCHN shake cultures for 3 days at 28 °C, when endogenous MnP is not expressed (*42*). Extracellular medium from the transformants was tested for MnP activity (*15*), and the transformant exhibiting the highest activity was selected for further study. Enzymes were purified from the extracellular medium by successive Phenyl Sepharose, Blue Agarose affinity, and MonoQ anion exchange chromatographies (*35*, *42*). The yields were comparable to those for previous variants and recombinant wild-type MnP (~2 mg·L^{-1}) (*34*, *35*, *42*, *45*). The Rz values of the purified enzymes were >4.

Sequence Analysis of E39D Genomic DNA. Genomic DNA was isolated from 3-day-old stationary cultures of the E39D transformant grown in HCHN medium. PCR amplification of the introduced *gpd*−*mnp1* construct was performed using a forward primer in the *gpd* promoter and a reverse primer in intron IV and exon III of the *mnp1* coding region. The 685-bp amplified fragment encoded the first 118 amino acids of the MnP1 protein. The fragment was sequenced and the E39D mutation identified. The introduced mutation was the only alteration found in the E39D genomic fragment versus the wild-type *mnp1* gene.

Spectral Analyses. Electronic absorbance maxima of the native and oxidized intermediates for the wild-type and variant MnP proteins were compared (data not shown). All of the spectra were stable for the duration of several successive scans (up to 30 s) and exhibited only slow autoxidation ($k < 1$ s^{-1}) thereafter, indicating that the enzymes were kinetically active and stable. Spectral maxima for the variant enzymes and their respective intermediates closely matched those of wild-type MnP, indicating no significant alterations in the heme environments of the variant MnPs.

Steady-State Kinetic Analyses. Steady-state parameters for the wild type and each of the variant enzymes (E39A, E39D, E35D, and DDE) are listed in Table 1. Constants for the E35D−E39D double variant were not calculated, since Mn oxidation by the enzyme was barely detectable (data not shown). Table 1 also lists the redetermined values for D179N, E39Q, and E35Q variants which were previously constructed (*34*, *35*). With the exception of the E39D variant, the changes in k_{cat} and K_m values for Mn^{II} were consistent with previous reports (*34*, *35*, *37*).

Table 1: Steady-State Kinetic Parameters for Wild-Type and Mutant MnPs[a]

	k_{cat} (s^{-1})	$K_m(Mn^{II})$ (mM)	$K_m(H_2O_2)$ (μM)	$k_{cat}/K_m(Mn^{II})$ ($M^{-1}s^{-1}$)	$k_{cat}/K_m(H_2O_2)$ ($M^{-1}s^{-1}$)
wtMnP	300	0.060	40	5.0×10^6	7.5×10^6
E39D	6.5	1.3	6.0	5.0×10^3	1.1×10^6
E39D[b]	410	0.036	54	1.1×10^7	7.6×10^6
E39Q	3.5	0.8	3.2	4.4×10^3	1.1×10^6
E39A	0.77	1.9	0.69	4.1×10^2	1.1×10^6
E35D	3.3	2.5	0.43	1.3×10^3	7.7×10^6
E35Q	0.83	3.8	0.5	2.2×10^2	1.7×10^6
D179N	2.87	2.0	1.6	1.4×10^3	1.8×10^6
DDE[c]	1.3	2.5	0.6	5.2×10^2	2.2×10^6

[a] Reactions contained 0.5 μg/mL enzyme in 50 mM malonate (pH 4.5). The ionic strength was adjusted to $\mu = 0.1$ M with K_2SO_4. Parameters for Mn^{II} were determined using 0.1 M H_2O_2. Parameters for H_2O_2 were determined using 5 mM $MnSO_4$. [b] From ref *37*. [c] DDE = the triple variant E35D−E39D−D179E.

The E39D variant we constructed showed markedly different kinetics from those previously reported for this variant (Table 1) (*37*). Our variant showed a 50-fold decrease in k_{cat} to 6.5 s^{-1} compared with the wild-type rate of 300 s^{-1} (*15*) and in contrast to the previous report citing no change in the k_{cat} value associated with this mutation versus the wild type (*37*). The k_{cat} values for the majority of the single ligand variants (D179A, D179N, E39Q, and E35D) decreased 50−100-fold, while several variants (E39A, E35Q, and DDE) showed 300−400-fold decreases in k_{cat}, in agreement with previous work (*34*, *35*, *37*).

Our E39D variant also showed a 20-fold increase in the K_m for Mn^{II} to approximately 1 mM, in contrast to the previously reported K_m of 36 μM for this same variant (*37*). Again, this 20-fold increase in K_m is consistent with the other single ligand variants, which all showed a 15−60-fold increase in the K_m for Mn^{II}. The resulting catalytic efficiency for Mn^{II} was decreased 10^3-fold for all of the variants except E39A, E35A, and DDE, for which the efficiency dropped 10^4-fold, again conflicting with the previous report citing no change in efficiency for the E39D variant (*37*). None of the variants exhibited changes in the catalytic efficiency for H_2O_2, in agreement with the previous report for E35D and in contrast with previous reports for the E39Q, E35Q, and D179N variants (*34*, *35*).

Formation of MnP Compound I. The rates of compound I formation for wild-type MnP and the E39D, E39A, E35D, and DDE variants were measured in 50 mM malonate at pH 4.5 by following the change in absorption of the enzyme at 397 nm, the isosbestic point between compound I and compound II. Kinetic traces, from which pseudo-first-order rate constants (k_{1obs}) were measured, displayed exponential character. Plots of k_{1obs} versus $[H_2O_2]$ were linear with zero ordinate intercepts, indicating irreversible second-order kinetics (data not shown). Apparent second-order rate constants for the variant MnPs were similar to the wild type and previously reported values for other binding site variants (*34*, *35*, *37*) (Table 2).

Table 2: Transient-State Kinetic Parameters: Apparent Second-Order Rate Constants (M^{-1} s^{-1}) for Formation and Reduction of Compound I[a]

	compound I formation	compound I reduction		
enzyme	H_2O_2	Mn^{II}	Br^-	$K_4Fe(CN)_6$
wild type	$(4.8 \pm 0.1) \times 10^6$	$\sim 3 \times 10^7$	$(2.7 \pm 0.5) \times 10^3$	$(4.8 \pm 0.1) \times 10^5$
E39D	$(4.4 \pm 0.7) \times 10^6$	$(1.3 \pm 0.1) \times 10^6$	$(2.4 \pm 0.1) \times 10^3$	$(4.8 \pm 0.1) \times 10^5$
E35D	$(5.1 \pm 0.1) \times 10^6$	$(4.7 \pm 0.2) \times 10^5$	$(2.4 \pm 0.1) \times 10^3$	$(4.5 \pm 0.1) \times 10^5$
E39A	$(4.9 \pm 0.1) \times 10^6$	$(8.3 \pm 0.2) \times 10^4$	$(1.6 \pm 0.1) \times 10^3$	$(3.6 \pm 0.1) \times 10^5$
DDE[b]	$(5.0 \pm 0.1) \times 10^6$	$(9.0 \pm 0.2) \times 10^4$	$(2.1 \pm 0.3) \times 10^3$	$(4.0 \pm 0.2) \times 10^5$

[a] Reaction mixtures contained 1 mM enzyme and 50 mM malonate (pH 4.5), final concentrations. The ionic strength of all solutions was adjusted to $\mu = 0.1$ M with K_2SO_4. Reactions were conducted under pseudo-first-order conditions, and substrate concentrations were varied as described in the text. Constants were determined from slopes of linear k_{obs} vs [S] plots. Individual kinetic traces showed exponential character and were fitted to obtain k_{obs}. [b] DDE = the triple variant E35D−E39D−D179E.

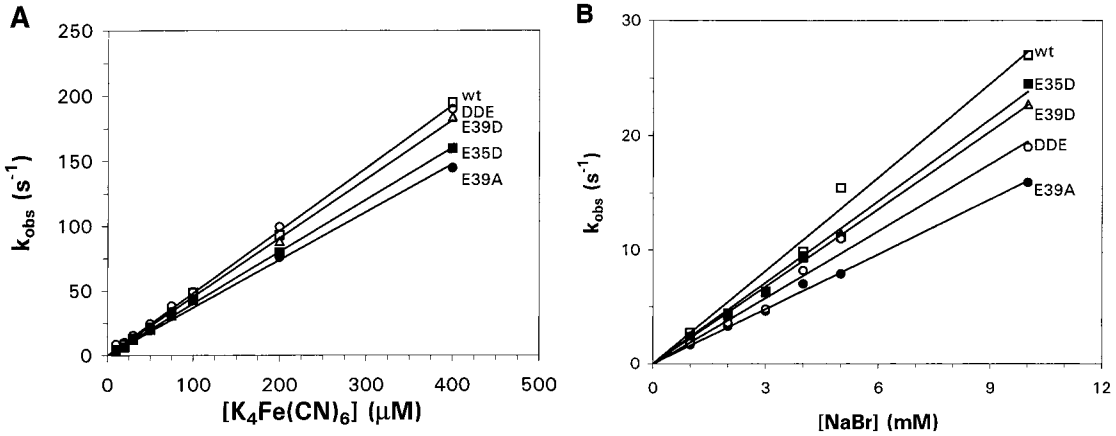

FIGURE 2: Kinetics of compound I reduction by ferrocyanide (A) and bromide (B). Wild-type (□), E39D (△), E35D (■), E39A (●), and DDE (E39D−E35D−D179E) (○). Reaction mixtures contained a final concentration of 1 μM enzyme and 50 mM malonate (pH 4.5). All kinetic traces displayed single-exponential character and were fitted to obtain k_{obs} values.

Reduction of MnP Compound I. Kinetic parameters for the reduction of compound I are listed in Table 2. Single-electron reductions of compound I to compound II of the variant enzymes by K_4FeCN_6 and Mn^{II} were examined in 50 mM malonate, pH 4.5, at 416 nm, the isosbestic point between compound II and native enzyme. The two-electron reduction of compound I to native enzyme by Br^- was followed at 406 nm. All kinetic traces used to calculate pseudo-first-order rate constants (k_{2obs}) were exponential in character, and plots of k_{2obs} versus substrate concentration were linear (Figures 2 and 3). The second-order rate constants for reduction of the variant MnPs by K_4FeCN_6 and Br^- were similar to wild-type MnP. However, second-order rate constants for reduction by Mn^{II} were significantly lower than wild-type MnP and varied considerably for the different variants. The rate constant for the E39D variant was ~30-fold lower than that of wild-type MnP and that previously reported for this variant (*37*). The rate constant for E35D was 100-fold lower than that of wild-type MnP and 10-fold lower than that previously reported for this variant (*37*). The rate constants for both the E39A single variant and the E35D−E39D−D179E triple variant were 1000-fold lower than that of wild-type MnP.

Reduction of MnP Compound II. Reduction of compound II by K_4FeCN_6 (Table 3) and Mn^{II} (Table 3) was measured in 50 mM malonate, pH 4.5, at 420 nm. Plots of k_{obs} versus Mn^{II} concentration exhibited saturation kinetics (Figure 4) as have been previously observed for wild-type MnP (*35*) and the E35D and E39D variants (*37*). Dissociation constants, K_D, and first-order rate constants, k_3, were determined as previously described (*15*) (Table 3). The K_D values increased

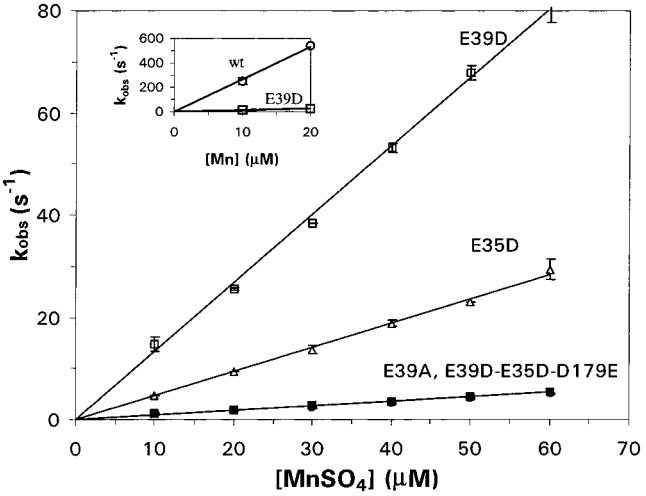

FIGURE 3: Kinetics of compound I reduction by Mn^{II}. E39D (□), E35D (△), E39A (■), and DDE (E39D−E35D−D179E) (●). The wild type (○) and E39D (□) are shown in the inset for comparison; note the difference in scale. Reaction mixtures contained a final concentration of 1 μM enzyme and 50 mM malonate, pH 4.5. All kinetic traces displayed single-exponential character and were fitted to obtain k_{obs} values.

10−80-fold while the k_{cat} value decreased 40-fold for the E39D variant, 120-fold for E35D, and 1200-fold for E39A, compared with the wild type. The calculated apparent second-order rate constants decreased 10^3−10^4-fold compared with wild-type MnP. Values for the E35D variant are in agreement with those previously reported for this variant, whereas the values for the E39D variant are in sharp contrast to the previous report that this mutation does not affect Mn binding or the rate of compound II reduction by Mn^{II} (*37*).

Table 3: Transient-State Kinetic Parameters for the Reduction of Compound II[a]

	$K_4Fe(CN)_6$	Mn^{II}		
enzyme	k_{3app} ($M^{-1}s^{-1}$)	k_3 (s^{-1})	K_D (M)	k_{3app} ($M^{-1}s^{-1}$)
wild type	$(7.8 \pm 0.2) \times 10^3$	$(5.6 \pm 0.1) \times 10^2$	$(1.1 \pm 0.3) \times 10^{-4}$	5.2×10^6
E39D	$(6.4 \pm 0.5) \times 10^3$	$(1.4 \pm 0.1) \times 10^1$	$(1.1 \pm 0.1) \times 10^{-3}$	9.4×10^3
E35D	$(6.6 \pm 0.4) \times 10^3$	$(4.8 \pm 0.5) \times 10^0$	$(8.1 \pm 1.7) \times 10^{-3}$	5.9×10^2
E39A	$(6.5 \pm 0.2) \times 10^3$	$(4.5 \pm 0.5) \times 10^{-1}$	$(1.8 \pm 0.1) \times 10^{-3}$	2.4×10^2
DDE[b]	$(7.0 \pm 0.2) \times 10^3$	$(4.0 \pm 0.3) \times 10^{-1}$	$(2.3 \pm 0.4) \times 10^{-3}$	1.7×10^2

[a] Reaction mixtures contained 1 μM enzyme and 50 mM malonate (pH 4.5), final concentrations. The ionic strength of all solutions was adjusted to $\mu = 0.1$ M with K_2SO_4. Reactions were conducted under pseudo-first-order conditions, and substrate concentrations were varied as described in the text. Constants were determined as described (*15*). Individual kinetic traces showed exponential character and were fitted to obtain k_{obs}. [b] DDE = the triple variant E35D−E39D−D179E.

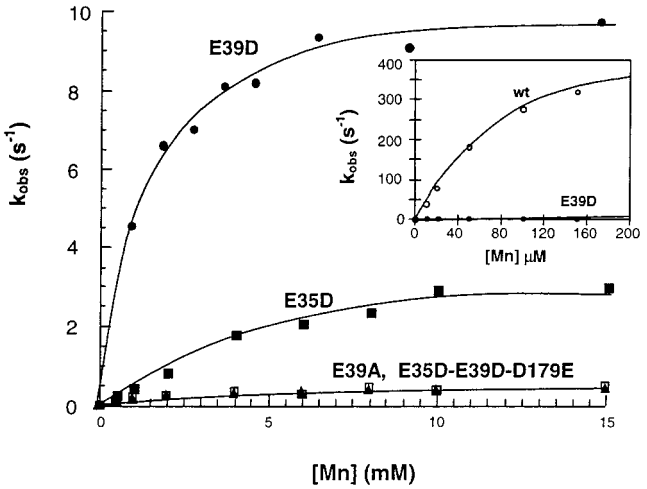

FIGURE 4: Kinetics of compound II reduction by Mn^{II}. E39D (●), E35D (■), DDE (E39D−E39D−D179E) (□), and E39A (▲). The wild type (○) and E39D (●) are shown in the inset for comparison; note the difference in scale. Reactions contained a final concentration of 1 μM enzyme and 50 mM malonate, pH 4.5. All kinetic traces displayed exponential character and were fitted to obtain k_{obs} values.

DISCUSSION

MnP is unique among Mn binding enzymes in its ability to bind and oxidize Mn^{II} and efficiently release Mn^{III}. This discriminatory binding is a critical aspect of MnP function. As a result of combined kinetic and crystallographic studies of these variants, the residues D179, E35, and E39 were identified as catalytically important Mn^{II} ligands (*19*, *34*−*36*). In the first set of binding site variants, the amino acid carboxylate ligands were exchanged for their respective amides via site-directed mutagenesis of the *mnp1* gene from *P. chrysosporium* (*34*, *35*). Since amides are poor ligands for Mn, these variants were designed to maintain steric constraints in the enzyme while selectively interfering with Mn ligation.

E39 is conserved in all known MnP sequences (*16*), and previous kinetic analyses (*35*) and the X-ray crystal structures (*19*, *36*) clearly indicate that E39 is, in fact, a ligand to the Mn. However, a more recent mutagenesis study using isochemical substitution of these ligands has raised doubts about the importance of E39 in Mn^{II} binding and oxidation (*37*). In that study, an E39D variant of MnP was constructed which was claimed to exhibit wild-type reaction kinetics for Mn^{II}. As a result, the authors proposed that E39 was not a ligand to the Mn. There are two alternate explanations for the proposed wild-type kinetics of the E39D variant in that study (*37*). The first is that the mutation was lost and the kinetics observed really are those of a wild-type enzyme. The second possibility concerns the isochemical nature of the substitution. In the E39D mutation, the functional carboxyl group is retained, although the side chain is shortened by one methylene group. It is possible that a shortened D39 residue could still ligate the Mn in a fashion similar to the original E39 residue, if there were some flexibility in the Mn binding site.

To further investigate this possibility, we first performed molecular modeling of the E39D and E35D variants. In the model, the Mn−ligand bond distances indicate that perhaps the mutated D35 residue is no longer capable of binding Mn, in agreement with the kinetic analysis of this variant (*37*). However, modeling of the E39D and E35D−E39D−D179E variants indicated possible flexibility in the binding site, whereby the mutated residues might still function as ligands, but only with an accompanying change in the Mn ligation geometry (Figure 1). If the ligation geometry of the variants was fixed into the wild-type, near-octahedral conformation, the metal−ligand bond distances were increased by 0.5−0.8 Å, resulting in probable loss of the mutated ligands.

To evaluate the models, we reconstructed the E39D and E35D variant MnPs using our homologous expression system (*42*). The results of our kinetic analysis of the E35D variant are very similar to those previously obtained (Tables 1−3) (*37*), which is significant since the variants were expressed in different systems. The previous E35D variant was heterologously expressed in *E. coli* and reconstituted with calcium and heme. The resulting enzyme was not glycosylated. In contrast, homologous expression in *P. chrysosporium* results in a fully processed and secreted enzyme which is glycosylated and which does not require reconstitution. The similar kinetic results for both the E35D variant MnPs in this work and the previous study (*37*) indicate that differences in the expression systems did not affect the overall kinetic characteristics of these variants.

Our results for the E39D variant, however, are markedly different from those of the previous study (*37*). Steady-state and transient-state analyses of our E39D variant MnP clearly indicate that the binding and oxidation of Mn^{II} are significantly reduced by this substitution. Sequencing of genomic DNA from the transformed fungus containing the recombinant gene indicated that the E39D mutation was correct with no other sequence alterations present. We also constructed an E39A mutation, effectively removing the ligand from the binding site. As expected, kinetic analysis indicates that the E39A substitution decreases Mn binding and oxidation to a similar but slightly greater extent than the E39D substitution.

Transient-state kinetics indicate similar changes (Tables 2 and 3). These results, combined with those for the previous E39Q variant, clearly indicate that E39 plays an important role in binding and oxidation of Mn^{II}.

In addition to the single-site substitutions, we constructed an E35D−E39D−D179E isochemical triple variant. In this variant, two of the ligand side chains were shortened while the third was lengthened. Molecular modeling indicated that this triple-substituted binding site might still be functional for Mn binding and oxidation if the Mn and associated water ligands were to move a few angstroms outward toward residues 35 and 39 (Figure 1D). Whereas the kinetics for Mn oxidation by the double variant (E35D−E39D) were barely measurable, the triple variant performed almost as well as the E39A single variant.

These combined results indicate that the Mn binding site may be relatively inflexible to changes in the geometry of the site. It appears that even isochemical substitutions greatly reduce both Mn binding and the rate of Mn oxidation. Although both the E39D and the isochemical triple variants are theoretically capable of Mn binding, both binding and electron transfer are in fact diminished. The kinetic data support the assertion that maintenance of the octahedral Mn ligation geometry predominates bond formation. The fact that the E39D variants perform slightly better than the E39A and E39Q variants and the E35D−E39D−D179E triple variant performs as well as a single variant indicates weak ligation in the altered sites. However, it is most likely energetically unfavorable for the Mn to adopt the altered geometry required for the substituted residues to act as good ligands. This is supported by crystal field theory in which tetragonally distortion of an octahedral complex is accompanied by electron spin pairing in the metal, which is energetically unfavorable for Mn (*47*).

Our results have interesting implications for attempts to engineer MnP-like Mn binding sites into other proteins. Recent studies with variants of cytochrome *c* peroxidase (CcP) engineered to contain an Mn binding site also indicate that precise geometry is required for efficient Mn binding and oxidation (*48*, *49*). Similar to our results for MnP, and despite promising modeling of the CcP variants, the best Mn binding CcP performed only as well as any of the single ligand MnP variants (*48*). The preference of Mn ions for octahedral ligation and the preferential differences in the binding geometries of Mn^{II} and Mn^{III} for carboxyl oxygens may prove important to the mechanism of the Mn binding site in MnP. While Mn^{II} can bind equally well in either the syn or the anti orientation, Mn^{III} prefers the anti orientation (*50*). Therefore, the exact orientation of ligands within the Mn site might directly affect binding of Mn^{II}, modulate the redox transition from Mn^{II} to Mn^{III}, or affect release of Mn^{III}.

In summary, mutation of the E39 residue in MnP decreases both Mn binding and oxidation as indicated by both steady-state and transient-state kinetics. The catalytic efficiency of the E39A (as shown herein) and E39Q (*35*) variants decreases $\sim 10^4$-fold, while that of the E39D variant decreases $\sim 10^3$-fold. These results clearly indicate that the E39 residue is a ligand to the Mn. We also investigated a E35D−E39D−D179E triple variant MnP which, despite favorable modeling studies, performed only as well as any of the single Mn ligand variants. The catalytic efficiency of the triple variant was decreased 10^4-fold, which is, however, $\sim 10^2$-fold better than that reported for a double variant MnP (*35*). These combined modeling and steady-state and transient-state kinetic studies indicate that precise geometry of the Mn ligands in the Mn binding site of MnP is essential for the efficient binding, oxidation, and release of Mn by this enzyme.

REFERENCES

1. Eriksson, K.-E. L., Blanchette, R. A., and Ander, P. (1990) *Microbial and Enzymatic Degradation of Wood and Wood Components*, Springer-Verlag, Berlin.
2. Sarkanen, K. V., and Ludwig, C. H. (1971) *Lignins. Occurrence, Formation, Structure and Reactions*, Wiley-Interscience, New York.
3. Buswell, J. A., and Odier, E. (1987) *CRC Crit. Rev. Biotechnol. 6*, 1−60.
4. Kirk, T. K., and Farrell, R. L. (1987) *Annu. Rev. Microbiol. 41*, 465−505.
5. Gold, M. H., Wariishi, H., and Valli, K. (1989) *ACS Symp. Ser. 389*, 127−140.
6. Hammel, K. E., Jensen, K. A., Jr., Mozuch, M. D., Landucci, L. L., Tien, M., and Pease, E. A. (1993) *J. Biol. Chem. 268*, 12274−12281.
7. Orth, A. B., Royse, D. J., and Tien, M. (1993) *Appl. Environ. Microbiol. 59*, 4017−4023.
8. Hatakka, A. (1994) *FEMS Microbiol. Rev. 13*, 125−135.
9. Homolka, L., Nerud, F., Kofronová, O., Novotná, E., and Machurová, V. (1994) *Folia Microbiol. (Prague) 39*, 37−43.
10. Pelaez, F., Martinez, M. J., and Martinez, A. T. (1995) *Mycol. Res. 99*, 37−42.
11. Périé, F. H., Sheng, D., and Gold, M. H. (1996) *Biochim. Biophys. Acta 1297*, 139−148.
12. Glenn, J. K., and Gold, M. H. (1985) *Arch. Biochem. Biophys. 242*, 329−341.
13. Kirk, T. K., Croan, S., Tien, M., Murtagh, K. E., and Farrell, R. L. (1986) *Enzyme Microb. Technol. 8*, 27−32.
14. Glenn, J. K., Akileswaran, L., and Gold, M. H. (1986) *Arch. Biochem. Biophys. 251*, 688−696.
15. Wariishi, H., Valli, K., and Gold, M. H. (1992) *J. Biol. Chem. 267*, 23688−23695.
16. Gold, M. H., Youngs, H. L., and Sollewijn Gelpke, M. D. (2000) in *Manganese and Its Role in Biological Processes* (Sigel, A., and Sigel, H., Eds.) pp 559−586, Marcel Dekker, New York.
17. Pribnow, D., Mayfield, M. B., Nipper, V. J., Brown, J. A., and Gold, M. H. (1989) *J. Biol. Chem. 264*, 5036−5040.
18. Godfrey, B. J., Mayfield, M. B., Brown, J. A., and Gold, M. H. (1990) *Gene 93*, 119−124.
19. Sundaramoorthy, M., Kishi, K., Gold, M. H., and Poulos, T. L. (1994) *J. Biol. Chem. 269*, 32759−32767.
20. Kunishima, N., Fukuyama, K., Matsubara, H., Hatanaka, H., Shibano, Y., and Amachi, T. (1994) *J. Mol. Biol. 235*, 331−344.
21. Petersen, J. F., Kadziola, A., and Larsen, S. (1994) *FEBS Lett. 339*, 291−296.
22. Schuller, D. J., Ban, N., Huystee, R. B., McPherson, A., and Poulos, T. L. (1996) *Structure 4*, 311−321.
23. Edwards, S. L., Raag, R., Wariishi, H., Gold, M. H., and Poulos, T. L. (1993) *Proc. Natl. Acad. Sci. U.S.A. 90*, 750−754.
24. Wariishi, H., Dunford, H. B., MacDonald, I. D., and Gold, M. H. (1989) *J. Biol. Chem. 264*, 3335−3340.
25. Kuan, I. C., Johnson, K. A., and Tien, M. (1993) *J. Biol. Chem. 268*, 20064−20070.
26. Kishi, K., Wariishi, H., Marquez, L., Dunford, H. B., and Gold, M. H. (1994) *Biochemistry 33*, 8694−8701.
27. Tuor, U., Wariishi, H., Schoemaker, H. E., and Gold, M. H. (1992) *Biochemistry 31*, 4986−4995.
28. Joshi, D. K., and Gold, M. H. (1993) *Appl. Environ. Microbiol. 59*, 1779−1785.
29. Joshi, D. K., and Gold, M. H. (1994) *Biochemistry 33*, 10969−10976.

30. Valli, K., Brock, B. J., Joshi, D. K., and Gold, M. H. (1992) *Appl. Environ. Microbiol. 58*, 221−228.
31. Valli, K., Wariishi, H., and Gold, M. H. (1992) *J. Bacteriol. 174*, 2131−2137.
32. Bao, W., Fukushima, Y., Jensen, K. A., Jr., Moen, M. A., and Hammel, K. E. (1994) *FEBS Lett. 354*, 297−300.
33. Wariishi, H., Valli, K., Renganathan, V., and Gold, M. H. (1989) *J. Biol. Chem. 264*, 14185−14191.
34. Kusters-van Someren, M., Kishi, K., Lundell, T., and Gold, M. H. (1995) *Biochemistry 34*, 10620−10627.
35. Kishi, K., Kusters-van Someren, M., Mayfield, M. B., Sun, J., Loehr, T. M., and Gold, M. H. (1996) *Biochemistry 35*, 8986−8994.
36. Sundaramoorthy, M., Kishi, K., Gold, M. H., and Poulos, T. L. (1997) *J. Biol. Chem. 272*, 17574−17580.
37. Whitwam, R. E., Brown, K. R., Musick, M., Natan, M. J., and Tien, M. (1997) *Biochemistry 36*, 9766−9773.
38. Alic, M., Clark, E. K., Kornegay, J. R., and Gold, M. H. (1990) *Curr. Genet. 17*, 305−311.
39. van Gunsteren, W. F. (1990) *Angew. Chem., Int. Ed. Engl. 29*, 992−1023.
40. Alic, M., Kornegay, J. R., Pribnow, D., and Gold, M. H. (1989) *Appl. Environ. Microbiol. 55*, 406−411.
41. Alic, M., Mayfield, M. B., Akileswaran, L., and Gold, M. H. (1991) *Curr. Genet. 19*, 491−494.
42. Mayfield, M. B., Kishi, K., Alic, M., and Gold, M. H. (1994) *Appl. Environ. Microbiol. 60*, 4303−4309.
43. Alic, M., Letzring, C., and Gold, M. H. (1987) *Appl. Environ. Microbiol. 53*, 1464−1469.
44. Youngs, H. L., Sundaramoorthy, M., and Gold, M. H. (2000) *Eur. J. Biochem. 267*, 1761−1769.
45. Sollewijn Gelpke, M. D., Moënne-Loccoz, P., and Gold, M. H. (1999) *Biochemistry 38*, 11482−11489.
46. Alic, M., Akileswaran, L., and Gold, M. H. (1997) *Biochim. Biophys. Acta 1338*, 1−7.
47. Cotton, F. A., and Wilkinson, G. (1980) *Advanced Inorganic Chemistry: A Comprehensive Text*, 4th ed., pp 647−650, John Wiley & Sons, New York.
48. Wilcox, S. K., Putnam, C. D., Sastry, M., Blankenship, J., Chazin, W. J., McRee, D. E., and Goodin, D. B. (1998) *Biochemistry 37*, 16853−16862.
49. Yeung, B. K., Wang, X., Sigman, J. A., Petillo, P. A., and Lu, Y. (1997) *Chem. Biol. 4*, 215−221.
50. Christianson, D. W. (1997) *Prog. Biophys. Mol. Biol. 67*, 217−252.

BI002104S